HHS Public Access

Author manuscript

Neurobiol Dis. Author manuscript; available in PMC 2021 October 01.

Published in final edited form as:

Neurobiol Dis. 2021 July ; 155: 105369. doi:10.1016/j.nbd.2021.105369.

Cell-intrinsic effects of TorsinA(ΔE) disrupt dopamine release in a mouse model of *TOR1A* dystonia

Anthony M. Downs, Ph.D..[a], **Xueliang Fan, Ph.D.**[a], **Radhika F. Kadakia, B.S.**[a], **Yuping Donsante, M.A.**[a], **H.A. Jinnah, M.D., Ph.D**[b,c,d], **Ellen J. Hess, Ph.D.**[a,b]

[a]Department of Pharmacology, Emory University School of Medicine, 101 Woodruff Circle, WMB 6304, Atlanta, GA 30322, USA

[b]Department of Neurology, Emory University School of Medicine, 101 Woodruff Circle, WMB 6304 Atlanta, GA 30322, USA

[c]Department of Human Genetics, Emory University School of Medicine, 101 Woodruff Circle, WMB 6300, Atlanta, GA 30322, USA

[d]Department of Pediatrics, Emory University School of Medicine, 101 Woodruff Circle, WMB 6300, Atlanta, GA 30322, USA

Abstract

TOR1A-associated dystonia, otherwise known as *DYT1* dystonia, is an inherited dystonia caused by a three base-pair deletion in the *TOR1A* gene (*TOR1A*ΔE). Although the mechanisms underlying the dystonic movements are largely unknown, abnormalities in striatal dopamine and acetylcholine neurotransmission are consistently implicated whereby dopamine release is reduced while cholinergic tone is increased. Because striatal cholinergic neurotransmission mediates dopamine release, it is not known if the dopamine release deficit is mediated indirectly by abnormal acetylcholine neurotransmission or if *Tor1a(ΔE)* acts directly within dopaminergic neurons to attenuate release. To dissect the microcircuit that governs the deficit in dopamine release, we conditionally expressed *Tor1a(ΔE)* in either dopamine neurons or cholinergic interneurons in mice and assessed striatal dopamine release using *ex vivo* fast scan cyclic voltammetry or dopamine efflux using *in vivo* microdialysis. Conditional expression of *Tor1a(ΔE)* in cholinergic neurons did not affect striatal dopamine release. In contrast, conditional expression of *Tor1a(ΔE)* in dopamine neurons reduced dopamine release to 50% of normal, which is comparable to the deficit in $Tor1a^{+/\Delta E}$ knockin mice that express the mutation ubiquitously. Despite the deficit in dopamine release, we found that the *Tor1a(ΔE)* mutation does not cause obvious nerve terminal dysfunction as other presynaptic mechanisms, including electrical excitability, vesicle recycling/refilling, Ca^{2+} signaling, D2 dopamine autoreceptor function and $GABA_B$ receptor function, are intact. Although the mechanistic link between *Tor1a(ΔE)* and dopamine release is unclear, these results clearly demonstrate that the defect in dopamine release is caused by the action of the *Tor1a(ΔE)* mutation within dopamine neurons.

Corresponding author: Ellen J. Hess, Departments of Pharmacology and Neurology, Emory University School of Medicine, 101 Woodruff Circle, WMB 6303, Atlanta, GA 30322, +1 404 727 4911. ellen.hess@emory.edu.

Declarations of interest: none

Keywords

fast scan cyclic voltammetry; DYT1; cholinergic interneurons; acetylcholine; TorsinA

INTRODUCTION

Dystonia is a movement disorder characterized by abnormal muscle contractions that cause debilitating abnormal postures and/or twisting movements.(Albanese et al., 2013) *TOR1A*-associated dystonia, otherwise known as *DYT1* dystonia, is caused by a 3 base-pair in-frame deletion (ΔGAG) in the *TOR1A* gene that causes a single glutamic acid deletion in the torsinA protein, torsinA(ΔE).(Ozelius et al., 1997; Ozelius et al., 1992) While the causal mutation for *TOR1A* dystonia has been known for some time, the functional link between the *TOR1A(ΔE)* mutation and dystonia remains unclear.

It is challenging to identify the neuroanatomical or cellular dysfunction that underlies *TOR1A* dystonia because it is not generally associated with a clear neuropathology or neurodegeneration of specific nuclei. However, abnormalities in striatal dopamine (DA) and acetylcholine (ACh) neurotransmission are consistently implicated in multiple forms of dystonia.(Eskow Jaunarajs et al., 2015; Wichmann, 2008) Increased striatal cholinergic tone was initially suspected as an underlying pathophysiology in dystonia, because anticholinergics are often effective treatments.(Burke et al., 1986) Indeed, abnormalities in striatal cholinergic neurotransmission are consistently observed in mouse models of dystonia,(Eskow Jaunarajs et al., 2015; Eskow Jaunarajs et al., 2019; Pappas et al., 2018; Pelosi et al., 2017; Pisani et al., 2006) including *TOR1A* which exhibit an increase in striatal cholinergic tone.(Scarduzio et al., 2017) Reduced striatal DA neurotransmission is implicated in a diverse range of dystonias, including: idiopathic focal dystonias, secondary dystonia, and inherited dystonias, including *TOR1A*.(Berman et al., 2013; Cornett et al., 2017; Correll et al., 2017; Furukawa et al., 1996; Ichinose and Nagatsu, 1999; Kurian et al., 2011; Mehta et al., 2015; Rilstone et al., 2013; Simonyan et al., 2013; Tolosa and Compta, 2006; Wijemanne and Jankovic, 2015) While dopaminergic drugs are generally not used to treat most dystonias, many case reports or small studies demonstrate some benefit from direct and indirect DA agonists. (Fan et al., 2018) Conclusive evidence is lacking as no large placebo-controlled double-blind crossover trials have been performed. The *TOR1A* gene is abundantly expressed in DA neurons of the substantia nigra pars compacta (SNc) and the concentrations of DA and DA metabolites are abnormal in patients carrying the *TOR1A*(ΔE) mutation.(Augood et al., 2004; Augood et al., 2002; Augood et al., 1999; Augood et al., 1998; Furukawa et al., 2000) Consistent with the abnormalities in DA handling observed in patients, striatal dopamine release is significantly reduced in multiple different mouse strains carrying the *Tor1a*(ΔE) mutation.(Balcioglu et al., 2007; Downs et al., 2019; Page et al., 2010)

Normal striatal function requires reciprocal interaction between DA and ACh neurotransmission.(Gonzales and Smith, 2015; Lester et al., 2010; Rizzi and Tan, 2017) Under normal conditions, ACh released by striatal cholinergic interneurons (ChIs) activates nicotinic acetylcholine receptors located on DA terminals, which adjust the probability of

DA release.(Rice and Cragg, 2004; Threlfell and Cragg, 2011; Zhang et al., 2009) In fact, we recently discovered that the non-selective muscarinic receptor antagonist trihexyphenidyl normalizes striatal DA release in a mouse model of TOR1A-associated dystonia via this mechanism.(Downs et al., 2019) Normally, DA released by nigrostriatal DA neurons activates D2 dopamine receptors expressed on ChIs to inhibit the firing rate of ChIs and reduce ACh release.(Yan et al., 1997) However, in mouse models of *TOR1A* dystonia, D2 DA receptor activation enhances ChI firing rates.(Pisani et al., 2006; Scarduzio et al., 2017; Sciamanna et al., 2009; Sciamanna et al., 2012b) It has been suggested that the resulting increase in extracellular ACh acts on nAChRs on DA terminals to alter DA release (Scarduzio et al., 2017), although nAChR function on DA terminals appears to be normal. (Downs et al., 2019) Because *Tor1a* is expressed in all cell types,(Augood et al., 1999; Augood et al., 1998; Oberlin et al., 2004) it is not known if the DA release deficit is caused indirectly by abnormal striatal ACh neurotransmission, or if it is the result of intrinsic effects of the *Tor1a(ΔE)* mutation in DA neurons. In this study, we used a genetic approach to conditionally express the *Tor1a(ΔE)* variant in striatal ChIs or DA neurons to dissect the microcircuit that governs the abnormal DA release and interrogated potential mechanisms underlying the *Tor1a(ΔE)*-induced reduction in DA release. We found that expression of the *Tor1a(ΔE)* mutation in DA neurons alone was sufficient to recapitulate abnormalities in DA release while expression of the *Tor1a(ΔE)* mutation in ChIs alone did not affect DA release.

MATERIALS AND METHODS

Animals

For the conditional *Tor1a(ΔE)* expression experiments, $Tor1a^{+/swap}$ mice ($Tor1a^{tm4.1Wtd}$/J; JAX #0208099) were bred with either heterozygous *DAT-cre* (JAX #006660) or *ChAT-cre* (JAX #031661) mice. The $Tor1a^{swap}$ allele carries a normal exon 5, which is flanked by loxP sites. Downstream of the normal exon 5 is another copy of exon 5, which carries the Δgag mutation.(Weisheit and Dauer, 2015) Without Cre recombinase expression, only the normal *Tor1a* gene is expressed. However, in the presence of Cre, the normal exon 5 is excised, which allows conditional expression of $Tor1a^{\Delta E}$ in the endogenous *Tor1a* gene in a cell-type specific manner (Fig 1). For all other experiments, knockin mice heterozygous for the *Tor1a(ΔE)* mutation ($Tor1a^{+/\Delta E}$) and control littermates ($Tor1a^{+/+}$) were used. All mice were inbred on C57BL/6J and were bred at Emory University. Both male and female mice between 10–14 weeks of age were used for all experiments and all experiments were balanced for sex. Animals were maintained on a 12 h light/dark cycle with *ad libitum* access to food and water. Mice were group housed with nestlets for environmental enrichment. Mice were genotyped using PCR with the following primers: $Tor1a^{\Delta E}$ (forward primer, GCTATGGAAGCTCTAGTTGG; reverse primer CAGCCAGGGCTAAACAGAG); $Tor1a^{swap}$ (forward primer, TCCTCCCCCAAGTACATCAG; reverse primer CATAGCTCAGCCGTCCAGTC); *DAT-cre* (common primer, TGGCTGTTGGTGTAAAGTGG; WT reverse primer GGACAGGGACATGGTTGACT; cre reverse primer, CCAAAAGACGGCAATATGGT); *ChAT-cre* (WT forward primer, GCAAAGAGACCTCATCTGTGGA; cre forward primer, TTCACTGCATTCTAGTTGTGGT; common reverse primer, GATAGGGGAGCAGCACACAG). All studies were carried out in accordance with the

National Institutes of Health Guidelines on the Care and use of Laboratory Animals, ARRIVE guidelines, and approved by the Institutional Animal Care and Use Committee at Emory University.

Fast scan cyclic voltammetry

Fast scan cyclic voltammetry (FSCV) was performed as previously described.(Downs et al., 2019) Mice were euthanized by cervical dislocation, and the brain was sectioned at 300μm using a vibratome in ice-cold, oxygenated sucrose artificial cerebral spinal fluid (aCSF) containing [in mM]: sucrose [194], NaCl [20], KCl [4.4], $CaCl_2$ [1.2], $MgCl_2$ [1.2], NaH_2PO_4 [1.2], $NaHCO_3$ [25], D-glucose [11] at pH 7.4. Coronal brain slices were collected in a holding chamber containing oxygenated, bicarbonate-buffered aCSF containing [in mM]: NaCl [126], KCl [2.45], $CaCl_2$ [2.4], $MgCl_2$ [1.2], NaH_2PO_4 [1.2], $NaHCO_3$ [25], D-glucose [11] and maintained at room temperature for 45–60 min before experiments began.

All FSCV recordings were conducted in the dorsolateral striatum. This region was selected because it receives innervation from the motor cortex.(Hintiryan et al., 2016) A striatal slice at ~ bregma +0.26 mm, where the anterior commissure is fused, was transferred to the recording chamber and perfused with oxygenated aCSF at 32°C. After a 30 min equilibration, a carbon fiber electrode was inserted approximately 50 μm into the surface of the slice and a bipolar tungsten stimulating electrode was placed approximately 200 μm away. DA release was evoked by either 1-pulse (600 μA, 4 ms pulse width) or 5-pulse 100 Hz electrical stimulation at 5 min inter-stimulus intervals to prevent rundown. The scan rate for voltammetry was 400 V/s from −0.4 V to 1.3 V to −0.4 V verses Ag/AgCl with a sampling rate of 10 Hz using a Chem-Clamp voltammeter-amperometer (Dagan Corporation, Minneapolis, MN, USA). FSCV experiments were conducted and analyzed using Demon voltammetry software (Wake Forest University).(Yorgason et al., 2011) All drugs were diluted in aCSF and bath applied for 10–20 mins before recordings commenced to allow for equilibration. For the Ca^{2+} dose-response experiment, aCSF was prepared without calcium. Ca^{2+} was then added from a 1M $CaCl_2$ stock solution to prepare the appropriate Ca^{2+} concentration. All electrodes were calibrated to known DA standards in aCSF using a custom-made flow cell.

Tissue monoamines

Mice were euthanized by cervical dislocation and striata were rapidly dissected, frozen on dry ice, and stored at −80 °C. For high performance liquid chromatography (HPLC) analysis of monoamines, tissue was homogenized in 100mM perchloric acid by probe sonication at 4°C and centrifuged at 10,000 g for 10 min. The supernatant was collected and filtered through 0.45 μm PVDF membranes prior to analysis. The cell pellet was solubilized in 2% SDS and protein concentrations were determined using a BCA assay (ThermoFisher, Waltham, MA, USA). Monoamines were measured using HPLC with electrochemical detection as previously described.(Egami et al., 2007) The HPLC system consisted of an ESAS MD-150 × 3.2 mm column, an ESA 5020 guard cell, and an ESA 5600A Coularray detector with an ESA 6210 detector cell (ESA, Bedford MA). The guard cell potential was 475 mV; and the analytical cell potentials were 175, 100, 350, and 450 mV. Samples were

eluted at a flow rate of 0.4 mL/min with a mobile phase composed of [in mM], [1.7] 1-octanesulfonic acid sodium, [75] NaH_2PO_4, 0.25% triethylamine, and 8% acetonitrile at pH 2.9. Monoamines were identified by both retention time and electrochemical profile and compared with known standards.

No-net flux microdialysis

Microdialysis was performed as previously described.(Song et al., 2012) Briefly, concentric microdialysis probes were manufactured in-house and calibrated with 100 ng/mL DA in aCSF containing [in mM]: NaCl [147], KCl [3.5], $CaCl_2$ [1.2], $MgCl_2$ [1.2], NaH_2PO_4 [1] at pH 7.0–7.4. Mice were anesthetized with isoflurane and the probe was implanted in the dorsal striatum (from bregma: anterior 0.6 mm, lateral 1.7 mm, and ventral 4.5 mm). The probe was perfused with aCSF at a flow rate of 0.6 μL/min while the mice habituated to the experimental chamber overnight. The following morning, the probe was perfused with aCSF and 0, 2, 10 or 20 nM DA (DA_{in}) presented in pseudo-random order. After a 30 min equilibration period for each concentration of DA, 3 samples (40 min each) were collected (DA_{out}). Samples were stored at −80 °C until HPLC analysis as described above. Extracellular DA levels were determined using simple linear regression analysis of the gain and loss of DA in the dialysate (DA_{in}-DA_{out}) versus DA_{in}. After sample collection, the probe location was verified by reverse dialysis of 3% bromophenol blue, and only mice with a probe correctly located in the dorsal striatum were included in the analysis.

Immunohistochemistry

Mice were euthanized with isoflurane, transcardially perfused with ice-cold normal saline followed by perfusion with ice-cold 4% paraformaldehyde in phosphate-buffered saline (PBS). Brains were removed and placed in 4% paraformaldehyde in PBS overnight at 4°C. Brains were then serially incubated in 20% and 30% sucrose solutions (w/v) for 24 hours each. Coronal sections were cut at 30 μm using a freezing microtome and stored in cryoprotectant at −20 °C.

Immunostaining for choline acetyltransferase (ChAT) or tyrosine hydroxylase (TH) was performed in free-floating sections were processed using the avidin-biotin complex method (ABC) (Vector Laboratories, Burlingame, CA, USA). Sections were washed in tris-buffered saline (TBS) and permeabilized with 0.4% Triton-X100 in TBS with 0.5% bovine serum albumin (BSA) for 10 mins. Sections were then incubated with 1% H_2O_2 for 30 mins to eliminate endogenous peroxidase activity. Sections were incubated in primary antibody using goat anti-ChAT 1:500 (Millipore cat # AB144P) or rabbit anti-TH 1:1000 (Pel-Freez cat # P4010–0) diluted in TBS containing 0.4% Triton-X100, 1% BSA and 5% normal donkey serum for 16 hours at 4°C with gentle agitation. Sections were then washed and incubated with biotinylated secondary antibody for 2 h and then incubated with the avidin-biotin complex reagent solution for 1 h. Chromogen was developed using the ImmPACT VIP peroxidase substrate kit (Vector). Sections were then mounted on charged slides and coverslipped.

Laser capture microdissection

Mice were euthanized by cervical dislocation, brains were rapidly removed, embedded in optimal cutting temperature solution (Sakura Fientek, Torrance, CA, USA) and frozen in a dry ice/isopentane slurry. Coronal sections were cut at 10 μm using a cryostat and sections containing the striatum and SNc/ventral tegmental area (VTA) were collected on Leica PET FrameSlides (Leica Microsystems, Buffalo Grove, IL, USA). Slides were stored at −80 °C until staining.

Immunostaining for ChAT or TH was performed using the following antibodies: rabbit anti-TH 1:200 (Pel-Freez cat # P4010–0) or goat anti-ChAT 1:25 (Millipore cat # AB144P). Sections were fixed in an acetone/methanol mixture (1:1) at −20 °C for 15 mins. Slides were washed in diethyl pyrocarbonate (DEPC)-treated water before incubation with primary antibody for 20 min at RT. Slides were then washed with DEPC-treated PBS before incubation with Alexa 488-conjugated secondary antibody for 5 min at RT. Slides were then washed in DEPC-treated PBS, treated with DAPI for 2 mins, and then washed with DEPC-treated PBS again. Slides were then dehydrated in graded ethanols and xylenes and then air dried. Slides proceeded immediately to laser capture microdissection (LCM). LCM was performed using an Arcturus XT Laser Capture Microdissection system (Thermo Fisher) with a Nikon Eclipse Ti-E microscope base (Nikon Instruments, Melville, NY, USA). Microdissection was performed using both an infrared laser and ultraviolet light. Samples were collected on CapSure HS LCM Caps (Thermo Fisher).

RNA isolation and sequencing

RNA isolation and purification were performed using the PicoPure RNA Isolation kit (Thermo Fisher). Briefly, a CapSure HS LCM cap containing microdissected cells was applied to a 0.5 mL microcentrifuge tube containing 10 μL extraction buffer and incubated for 30 min at 42°C. 10 μL of 70% ethanol was then added and mixed thoroughly. RNA was then purified using a nucleic acid binding column with on-column DNase treatment (RNase-free DNase set, QIAGEN, Germantown, MD, USA). RNA was then eluted from the column in elution buffer.

RNA was reverse transcribed using LunaScript RT SuperMix Kit (New England Biolabs, Ipswich, MA, USA). To confirm that striatal ChIs or midbrain dopaminergic neurons were collected via LCM, RT-qPCR was performed using Luna Universal qPCR master mix (New England Biolabs) with primers specific to 18s rRNA (forward primer 5’-GGACCAGAGCGAAAGCATTTGCC-3’ and reverse primer 5’-TCAATCTCGGGTGGCTGAACGC-3’), ChAT (forward primer 5’-GTGAGACCCTGCAGGAAAAG-3’ and reverse primer 5’-GCCAGGCGGTTGTTTAGATA-3’), or TH (forward primer 5’-GGTATACGCCACGCTGAAGG-3’ and reverse primer 5’-TAGCCACAGTACCGTTCCAGA-3’). To verify cell-type specific recombination of the *Tor1a*$^{+/swap}$ allele, cDNA encompassing the *Tor1a(Δgag)* mutation was amplified using forward primer 5’-GCCGTGTCGGTCTTCAATAA-3’ and reverse primer 5’-ACAGTCTTGCAGCCCTTGTC-3’. The PCR product was purified using QIAquick PCR purification kit (QIAGEN) and sequenced using the primer 5’-

GCCGTGTCGGTCTTCAATAA-3'. This primer is located within exon 4 of the *Tor1a* gene to ensure that cDNA derived from mRNA, but not genomic DNA was sequenced. Sequencing chromatographs were analyzed using 4Peaks software (Mekentosj, Amsterdam, NL).

Image collection

Slides were imaged under bright field illumination using an Olympus BX51 camera equipped with an Olympus DP72 camera and Olympus CellSens software. The same optical settings were used for image acquisition in each region from each mouse.

Statistical analysis

Data are presented as means with standard error. For all FSCV experiments, we used one slice per animal, so all samples are independent. Dose responses were analyzed with non-linear regression to determine EC_{50} or IC_{50}. IC_{50} and EC_{50} were analyzed using two-tailed Student's *t*-test. All other data were analyzed using one-way ANOVA with *post hoc* Dunnett's multiple comparison test or two-way ANOVA with Sidak's multiple comparisons test. All analyses were performed using Graphpad Prism 8 (https://www.graphpad.com/). Statistical significance was defined as $*p < 0.05$, $**p < 0.01$, $***p < 0.001$.

Compounds

Quinpirole and CGP 88584 were purchased from Tocris (Minneapolis, MN, USA).

RESULTS

Conditional expression of *Tor1a(ΔE)* in striatal ChIs does not affect striatal DA release

Because ChI dysfunction is implicated in *TOR1A* dystonia and cholinergic neurotransmission plays a critical role in regulating DA release,(Eskow Jaunarajs et al., 2015; Eskow Jaunarajs et al., 2019; Pappas et al., 2018; Threlfell et al., 2010; Threlfell and Cragg, 2011) we hypothesized that expression of *Tor1a(ΔE)* in striatal ChIs mediates the deficit in striatal DA release. To test this hypothesis, we generated mice that were heterozygous knockin for the $Tor1a^{+/\Delta E}$ mutation only in cholinergic neurons while other cells harbored the normal ($Tor1a^{+/+}$) alleles. To produce this cell-type specific genocopy of the human disease-causing genotype ($TOR1A^{+/\Delta E}$), we bred ChAT-cre mice, which drives Cre recombinase only in neurons that also express the choline acetyltransferase gene, onto the $Tor1a^{swap}$ mouse strain (*ChAT-cre;* $Tor1a^{+/swap}$ mice). To validate conditional expression of *Tor1a(ΔE)* in only ChIs, we used LCM to dissect ChAT-positive ChIs and sequenced the *Tor1a* gene from cDNA derived from these cells. The sequencing demonstrated heterozygous expression of *Tor1a(ΔE)* in ChIs but not ChAT-negative cells from the striatum in *ChAT-cre;* $Tor1a^{+/swap}$ mice nor in ChIs collected from *ChAT-cre;* $Tor1a^{+/+}$ mice (Fig 2A). As additional confirmation that ChIs were collected by LCM, we performed RT-qPCR for ChAT and found significant enrichment of ChAT transcripts in putative ChIs compared to other LCM-captured striatal cells where no ChAT immunostaining was detected (data not shown). Further, ChAT immunostaining in the dorsolateral CPu of *ChAT-cre;* $Tor1a^{+/swap}$ mice was indistinguishable from *ChAT-cre;* $Tor1a^{+/+}$ mice (Fig 2B).

We assessed total tissue striatal monoamine concentrations in *ChAT-cre; Tor1a*$^{+/swap}$ mice and control genotypes including *Tor1a*$^{+/swap}$ and *ChAT-cre; Tor1a*$^{+/+}$ to determine if expression of *Tor1a(ΔE)* in cholinergic neurons alone affected dopamine neurochemistry. Consistent with our previous work demonstrating that DA and DA metabolite concentrations are normal in *Tor1a*$^{+/ΔE}$ knockin mice,(Song et al., 2012) we found that there were no significant differences in the striatal concentrations of DA (one-way ANOVA, $F_{2,14}$ = 0.5173, p = 0.61), DOPAC ($F_{2,14}$ = 0.04246, p = 0.96), HVA ($F_{2,14}$ = 0.4396, p = 0.65), or 3-MT ($F_{2,14}$ = 0.6304, p = 0.63), among *Tor1a*$^{+/swap}$, *ChAT-cre; Tor1a*$^{+/+}$, or *ChAT-cre; Tor1a* $^{+/swap}$ mice (Table 1).

To determine if expression of the disease-causing genotype in cholinergic neurons was sufficient to induce a deficit in DA release, FSCV was used to measure evoked DA release in the dorsal striatum after single-pulse electrical stimulation. DA was identified by its characteristic oxidation peak at +600mV and reduction peak at −200mV (data not shown). There was no significant difference between the kinetics of DA uptake *ChAT-cre; Tor1a*$^{+/+}$ and *ChAT-cre; Tor1a*$^{+/swap}$ based on tau (*ChAT-cre; Tor1a*$^{+/+}$ 0.73 ± 0.03 s; *ChAT-cre; Tor1a* $^{+/swap}$ 0.78 ± 0.07 s, Student's *t* test, p = 0.57) (Fig 2C). Similarly, there was no significant difference in peak DA release between *ChAT-cre; Tor1a*$^{+/swap}$ and the control genotypes *Tor1a*$^{+/+}$, *Tor1a*$^{+/swap}$ and *ChAT-cre; Tor1a*$^{+/+}$ (Fig 2D). As we have shown previously, *Tor1a* $^{+/ΔE}$ knockin mice, which we used as a positive control, exhibited a significant reduction in DA release compared to *Tor1a*$^{+/+}$ mice. DA release in *Tor1a*$^{+/ΔE}$ knockin mice was also significantly reduced compared to *ChAT-cre; Tor1a*$^{+/swap}$ (*Tor1a*$^{+/ΔE}$, 0.91 ± 0.08 μM DA; *ChAT-cre; Tor1a*$^{+/swap}$, 1.66 ± 0.14 μM DA, $F_{4,32}$ = 10.54, $p < 0.0001$; Dunnet's multiple comparisons test, $p = 0.0013$) and all other genotypes. We also examined *in vivo* extracellular striatal DA after conditional expression of *Tor1a(ΔE)* in ChIs using no-net flux microdialysis. There was no significant difference in extracellular DA concentrations between *ChAT-cre; Tor1a*$^{+/+}$ and *ChAT-cre; Tor1a*$^{+/swap}$ (*ChAT-cre; Tor1a*$^{+/+}$ 4.15 ± 0.80 nM DA; *ChAT-cre; Tor1a*$^{+/swap}$ 4.51 ± 1.0 nM DA, Student's *t* test, p = 0.78, n = 7).

Conditional expression of *Tor1a(ΔE)* in DA neurons causes abnormal DA release

Because expression of the *Tor1a(ΔE)* mutation in cholinergic neurons had no effect on striatal DA release, we next hypothesized that the *Tor1a(ΔE)* mutation acts intrinsically within DA neurons to cause the deficit in DA release. To test this, DAT-cre, which drives Cre recombinase only in neurons that also express the DA transporter, was bred onto the *Tor1a*^{swap} mouse strain (*DAT-cre; Tor1a*$^{+/swap}$ mice). To validate conditional expression of *Tor1a(ΔE)* in only midbrain DA neurons, we used LCM to dissect TH-positive DA neurons and sequenced the *Tor1a* gene from cDNA derived from these cells. The sequencing demonstrated heterozygous expression of *Tor1a(ΔE)* in TH-positive neurons from *DAT-cre; Tor1a*$^{+/swap}$ mice but TH-negative cells and TH-positive DA neurons collected from *DAT-cre; Tor1a*$^{+/+}$ mice expressed only the normal *Tor1a* transcript (Fig 3A). We further validated that DA neurons were collected by using RT-qPCR for TH and found significant enrichment of TH transcripts in putative DA neurons versus other cells (data not shown). Further, TH immunostaining in midbrain DA neurons in *DAT-cre; Tor1a*$^{+/swap}$ mice was indistinguishable from *DAT-cre; Tor1a*$^{+/+}$ mice (Fig 3B).

To determine if conditional expression of the *Tor1a*(ΔE) mutation in DA neurons affected DA neurochemistry, we assessed total striatal monoamine concentrations. There were no significant differences in the striatal concentrations of DA (One-way ANOVA, $F_{2,15}$ = 0.8622, p = 0.44), DOPAC ($F_{2,15}$ = 0.2256, p = 0.80), HVA ($F_{2,15}$ = 0.5351, p = 0.53), or 3-MT ($F_{2,15}$ = 1.315, p = 0.30) among *Tor1a*$^{+/swap}$, *DAT-cre; Tor1a*$^{+/+}$, or *DAT-cre; Tor1a* $^{+/swap}$ mice (Table 1).

We then used FSCV to measure DA release evoked by single-pulse electrical simulation in the dorsolateral striatum after conditional expression of *Tor1a(ΔE)* in DA neurons. There was a significant reduction in peak DA release in *DAT-cre; Tor1a*$^{+/swap}$ relative to *DAT-cre; Tor1a*$^{+/+}$ and *Tor1a*$^{+/swap}$ (One-way ANOVA, $F_{4,32}$ = 11.24, p<0.0001; Dunnett's *post hoc* test, p = 0.008) (Fig 3C). There was no change in the kinetics of DA uptake between *DAT-cre; Tor1a*$^{+/+}$ and *DAT-cre; Tor1a*$^{+/swap}$ (*DAT-cre; Tor1a*$^{+/+}$ 0.78 ± 0.06 s; *DAT-cre; Tor1a* $^{+/swap}$ 0.67 ± 0.08, Student's *t* test, p = 0.33). The decrement in DA release in *DAT-cre; Tor1a*$^{+/swap}$ mice, which express the mutation in only DA neurons, was comparable to that of *Tor1a*$^{+/\Delta E}$ knockin mice, which express the mutation in all cell types (*DAT-cre; Tor1a* $^{+/swap}$, 0.94 ± 0.07 μM DA; *Tor1a*$^{+/\Delta E}$, 0.91 ± 0.08 μM DA, Dunnet's multiple comparison's test, p = 0.99) (Fig 3D) We also examined striatal extracellular DA concentrations *in vivo* in awake behaving *DAT-cre; Tor1a*$^{+/swap}$ and control mice using no-net-flux microdialysis. Extracellular DA was significantly reduced in *DAT-cre; Tor1a*$^{+/swap}$ versus *DAT-cre; Tor1a* $^{+/+}$ (*DAT-cre; Tor1a*$^{+/+}$ 5.36 ± 0.03 nM DA; *DAT-cre; Tor1a*$^{+/swap}$ 2.90 ± 0.55 nM DA, Student's *t* test, p = 0.048, n = 8). Overall, these results demonstrate that expression of the *Tor1a(ΔE)* in DA neurons causes a reduction in DA release without affecting DA neurochemistry.

Effects of the *Tor1a(ΔE)* mutation on the excitability of DA terminals

Our results suggest that the decrement in DA release is caused by intrinsic effects of the *Tor1a(ΔE)* on midbrain DA neurons, but the mechanisms underlying the DA release defect are unknown. To determine if abnormal excitability could account for the deficit in release, we conducted a current-response experiment using FSCV in global *Tor1a*$^{+/\Delta E}$ knockin and *Tor1a*$^{+/+}$ control mice. Stimulation current was varied between 200 μA and 800 μA and peak DA release was measured relative to our standard paradigm of 600 μA stimulation current (example DA-time traces after single-pulse 600 μA electrical stimulation, Fig 4A inset). The EC_{50} was comparable between control and *Tor1a*$^{+/\Delta E}$ knockin mice (EC_{50}: *Tor1a*$^{+/+}$ = 405.5 ± 8.73 μA; *Tor1a*$^{+/\Delta E}$ = 405.3 ± 6.11 μA; Student's *t*-test, p = 0.99, n=3; Fig 4A). Further, when the data were expressed as raw [DA], DA release in *Tor1a*$^{+/\Delta E}$ was reduced at all stimulation currents tested, except for the lowest stimulation currents between 200–300 μA which produced no DA release, and even the highest stimulation current did not overcome the deficit in DA release observed in *Tor1a*$^{+/\Delta E}$ knockin mice (Fig 4B).

Sensitivity to extracellular Ca^{2+} concentration in *Tor1a*$^{+/\Delta E}$ mice

Previous studies have shown that striatal DA release is highly sensitive to extracellular Ca^{2+} concentration and mediated by $Ca_V2.2$ channels.(Brimblecombe et al., 2015) Further, abnormal $Ca_V2.2$ Ca^{2+} channel activation has been observed in a transgenic mouse model carrying the *Tor1a(ΔE)* mutation suggesting that the regulation of release by Ca^{2+} is

abnormal in *Tor1a*$^{+/\Delta E}$ mice.(Pisani et al., 2006) To test this hypothesis, we assessed DA release in response to varying concentrations of Ca^{2+} (0–4mM Ca^{2+}) in global *Tor1a*$^{+/\Delta E}$ knockin and *Tor1a*$^{+/+}$ control mice after single-pulse electrical stimulation. There was no difference in the sensitivity to Ca^{2+} between genotypes with 1-pulse stimulation (Fig 4C) (EC_{50}: *Tor1a*$^{+/+}$ = 2.12 ± 0.21 mM; *Tor1a*$^{+/\Delta E}$ = 1.75 ± 0.36 mM; Student's *t*-test, p = 0.056, n=6). There was also no significant difference in the Hill slope between the genotypes indicating there is no alteration in cooperativity for Ca^{2+} (Hill coefficient: *Tor1a*$^{+/+}$ = 2.92 ± 0.60; *Tor1a*$^{+/\Delta E}$ = 2.95 ± 0.76; Student's *t*-test, p = 0.98 n=6). We also tested the effect of altered Ca^{2+} concentration on 5-pulse 100 Hz stimulations, because experimental manipulations of Ca^{2+} transients have strong frequency-dependent effects on DA release. (Brimblecombe et al., 2015; Zhang et al., 2009) We found no difference in EC_{50} or Hill slope after 5-pulse 100Hz stimulations (Fig 4D) (EC_{50}: *Tor1a*$^{+/+}$= 3.05 ± 2.45 mM; *Tor1a*$^{+/\Delta E}$ = 1.49 ± 0.43 mM; Student's *t*-test, p = 0.54, n=6; Hill coefficient: *Tor1a*$^{+/+}$ = 1.16 ± 0.37; *Tor1a*$^{+/\Delta E}$ = 1.94 ± 0.81; Student's *t*-test, p = 0.40 n=6).

Vesicle utilization in *Tor1a*$^{+/\Delta E}$ mice

Snapin, which interacts with SNARE proteins, has been implicated as an interacting partner with torsinA.(Granata et al., 2008; Misbahuddin et al., 2005) Abnormalities in docking proteins can disrupt the vesicle refilling rate (i.e., the restoration of the readily releasable pool of vesicles after a release event) suggesting that the reduction in DA release in *Tor1a*$^{+/\Delta E}$ knockin mice may result from sub-optimal vesicle utilization.(Kile et al., 2010) To test this hypothesis, we conducted a rundown experiment by applying electrical stimulation at varying inter-pulse intervals (IPI) (5 min, 3 min, 1 min, 10 sec, 0.3 sec IPI) and examined the rate of decline in peak DA release in global *Tor1a*$^{+/\Delta E}$ knockin and *Tor1a*$^{+/+}$ control mice. While long inter-stimulus intervals produced only moderate reductions in DA release (Fig 5A–C), DA release rapidly decreased at shorter inter-stimulus intervals of 10 s (Fig 5D) and 0.3 s intervals (Fig 5E; two-way ANOVA main effect of pulse number, $F_{3,30} = 131.1$, $p < 0.0001$). There was no difference between *Tor1a*$^{+/+}$ and *Tor1a*$^{+/\Delta E}$ mice (two-way ANOVA main effect of genotype, $F_{1,10} = 0.0017$, p = 0.97) at the 0.3s interval. To obtain the rate of run-down, we plotted the DA released at the second pulse normalized to the first pulse at all stimulation intervals (Fig 5F). There was no difference in the rate of rundown between *Tor1a*$^{+/+}$ and *Tor1a*$^{+/\Delta E}$ mice (two-way ANOVA genotype x IPI interaction effect, $F_{4,40} = 0.766$, p = 0.55).

D2 DA autoreceptor function in *Tor1a*$^{+/\Delta E}$ mice

D2 DA autoreceptors located on the terminals of nigrostriatal neurons negatively regulate extracellular DA concentrations by mediating release.(Bello et al., 2011; Koeltzow et al., 1998) A significant reduction in striatal D2 DA receptor availability is observed in human *TOR1A* carriers but it is not known whether these defects are associated with autoreceptors, postsynaptic receptors or both.(Asanuma et al., 2005; Carbon et al., 2009) To determine if abnormal D2 DA autoreceptor function mediates the deficit in DA release observed in *Tor1a*$^{+/\Delta E}$ mice, we assessed the effect of the D2 DA receptor agonist quinpirole on DA release in global *Tor1a*$^{+/\Delta E}$ knockin and *Tor1a*$^{+/+}$ control mice after single-pulse electrical stimulation (Fig 6A). Quinpirole dose-dependently decreased DA release in both genotypes, and there

was no significant difference in IC_{50} between *Tor1a*$^{+/+}$ and *Tor1a*$^{+/\Delta E}$ mice (IC_{50}: *Tor1a*$^{+/+}$ = 87.59 ± 22.01 μM; *Tor1a*$^{+/\Delta E}$ = 102.5 ± 39.97 μM; Student's *t*-test, p= 0.43 n=5).

$GABA_B$ receptor function in *Tor1a*$^{+/\Delta E}$ mice

Activation of $GABA_B$ receptors on DA terminals reduces DA release in slice.(Lopes et al., 2019) Further, a recent study demonstrated that enhanced GABA tone in slice can mediate a ~50% reduction in DA release similar to that observed in *Tor1a*$^{+/\Delta E}$ knockin mice.(Roberts et al., 2020) To determine if increased $GABA_B$ receptor activation and/or increased GABA tone mediates the reduction in DA release in *Tor1a*$^{+/\Delta E}$ knockin mice, we performed a dose response experiment with the selective $GABA_B$ antagonist CGP 88584 in global *Tor1a*$^{+/\Delta E}$ knockin and *Tor1a*$^{+/+}$ control mice after single-pulse electrical stimulation. CGP 88584 dose-dependently enhanced DA release in both *Tor1a*$^{+/+}$ and *Tor1a*$^{+/\Delta E}$ mice (Fig 6B). However, there was no significant difference in either EC_{50} (EC_{50}: *Tor1a*$^{+/+}$ = 1.16 ± 0.78 μM; *Tor1a*$^{+/\Delta E}$ = 0.66 ± 0.39 μM; Student's *t*-test, p = 0.58 n=5) or maximum effect between the genotypes at the highest drug concertation (10 μM CGP 88584) (main effect of treatment, two-way repeated measures ANOVA $F_{1,8}$ = 36.24, p = 0.0003, genotype x treatment interaction effect, $F_{1,8}$ = 3.85, p = 0.085) (Fig 6C).

DISCUSSION

Here, we demonstrate that the deficit in striatal DA release induced by *Tor1a(ΔE)* is caused by cell-intrinsic effects of the mutation within DA neurons while selective expression of *Tor1a(ΔE)* in striatal ChIs plays little, if any, role. Our results are in general agreement with a previous study demonstrating that transgenic overexpression of human torsinA(ΔE) in midbrain DA neurons causes a defect in DA release.(Page et al., 2010) However, in this same carefully-controlled study, overexpression of normal human torsinA also reduced striatal DA content, suggesting that overexpression, rather than the mutation *per se*, may have contributed to the abnormal dopaminergic response as it is known that overexpression of torsinA can produce extraneous CNS abnormalities that are unrelated to the mutation. (Grundmann et al., 2007) Here, we expressed the human disease-causing genotype (*Tor1a*$^{+/\Delta E}$) in midbrain DA neurons via the endogenous gene, thus avoiding the confound of transgenic overexpression, to unambiguously pinpoint the site of dysfunction as DA neurons using both *in vitro* and *in vivo* approaches.

Although striatal cholinergic and dopaminergic signaling are inextricably linked, we found that selective expression of the disease-causing genotype (*Tor1a*$^{+/\Delta E}$) in cholinergic neurons did not influence DA release in the striatum. Our results are consistent with a previous study that found that selective knockout of *Tor1a* (*Tor1a*$^{-/-}$) from cholinergic neurons does not affect the psychostimulant-induced increase in extracellular striatal DA.(Sciamanna et al., 2012a) Taken together these findings are surprising because while cholinergic tone appears to be abnormal in *Tor1a*$^{+/\Delta E}$ mice, it has little effect on DA neurotransmission.(Downs et al., 2019; Scarduzio et al., 2017) It is possible that either the alteration in ACh tone is not due to direct action of *Tor1a(ΔE)* in ChIs and/or that abnormal cholinergic neurotransmission caused by the mutation is not sufficient to appreciably impact DA release.

While our results demonstrate that intrinsic effects of *Tor1a(ΔE)* on DA neurons cause the deficit in DA release, the mechanism underlying this defect is unclear. Striatal tissue DA levels and the levels of DA metabolites in *DAT-cre; Tor1a*$^{+/swap}$ were normal, which is in agreement with our previous results in *Tor1a*$^{+/\Delta E}$ knockin mice.(Song et al., 2012) Because our *ex vivo* brain slice preparation lacks DA neuron cell bodies, the mechanism leading to reduced DA release cannot be explained by firing rates. Although the localization of torsinA within neurons is debated, (Augood et al., 2003; Koh et al., 2013; Puglisi et al., 2013) torsinA and its activators LAP1 and LULL1 appear to be localized to the nuclear membrane and endoplasmic reticulum.(Goodchild et al., 2015; Goodchild et al., 2005) Thus, it is reasonable to postulate that the *Tor1a(ΔE)*-induced reduction in DA release is not likely caused by direct action of *Tor1a(ΔE)* at the presynaptic terminal considering that, with the exception of the robust reduction in the amount of DA released, gross morphology and DA terminal function was largely intact.

Our results do offer clues to potential mechanisms that mediate the *Tor1a(ΔE)*-induced reduction in striatal DA release. *Tor1a(ΔE)* may disrupt DA release indirectly by disrupting basic cellular machinery in DA cell bodies. *Tor1a* has been linked with a variety of different cellular process, including: membrane protein trafficking, secretory protein processing, endoplasmic reticulum stress response, lipid metabolism, nuclear membrane function and maintenance, and many others.(Beauvais et al., 2018; Cascalho et al., 2020; Chen et al., 2010; Gonzalez-Alegre and Paulson, 2004; Goodchild and Dauer, 2004; Goodchild et al., 2005; Grillet et al., 2016; Hewett et al., 2000; Hewett et al., 2007; Torres et al., 2004) The strong link between *Tor1a* and endoplasmic reticulum function suggests the hypothesis that mutant *Tor1a(ΔE)* disrupts posttranslational processing of synaptic proteins or disrupts the lipid constitution of vesicles and/or cell membrane to reduce the probability of release. Alternatively, *Tor1a(ΔE)* may disrupt the normal development of DA neurons. For example, *Tor1a(ΔE)* may result in a decrease in the number of DA release sites in the striatum. While the cellular processes that regulate the number of DA release sites are poorly understood, it is possible that *Tor1a(ΔE)* reduces the number of striatal DA release sites by modulating glia-derived neurotrophic factor GDNF, which is known to enhance striatal DA release sites. (Kumar et al., 2015)

Taken together, our results demonstrate that the reduction in striatal DA release observed in mouse models of *TOR1A* dystonia is due to intrinsic effects of *Tor1a(ΔE)* on midbrain DA neurons and not ChIs. While the precise mechanism linking *Tor1a(ΔE)* to reduced DA release remains unknown, these results point to DA neurons as a cellular target for new therapeutics.

ACKNOWLEDGMENTS

This research project was supported in part by the Emory University Integrated Cellular Imaging Core and the Emory HPLC Bioanalytical Core.

FUNDING

This work was supported by United States Department of Defense grants W81XWH-15-1-0545 and W81XWH-20-1-0446, United States National Institute of Health Grants F31 NS103363 and T32 GM008602, and Cure Dystonia Now.

Abbreviations:

ACh	acetylcholine
aCSF	artificial cerebrospinal fluid
BSA	bovine serum albumin
ChAT	choline acetyltransferase
ChI	cholinergic interneuron
DA	dopamine
DEPC	diethyl pyrocarbonate
FSCV	fast scan cyclic voltammetry
HPLC	high performance liquid chromatography
IPI	inter-pulse interval
LCM	laser capture microdissection
PBS	phosphate-buffered saline
SNc	substantia nigra pars compacta
TBS	tris-buffered saline
TH	tyrosine hydroxylase
VTA	ventral tegmental area

REFERENCES

Albanese A, et al., 2013. Phenomenology and classification of dystonia: a consensus update. Mov Disord. 28, 863–73. [PubMed: 23649720]

Asanuma K, et al., 2005. Decreased striatal D2 receptor binding in non-manifesting carriers of the DYT1 dystonia mutation. Neurology. 64, 347–9. [PubMed: 15668438]

Augood SJ, et al., 2004. Dopamine transmission in DYT1 dystonia. Adv Neurol. 94, 53–60. [PubMed: 14509654]

Augood SJ, et al., 2002. Dopamine transmission in DYT1 dystonia: a biochemical and autoradiographical study. Neurology. 59, 445–8. [PubMed: 12177384]

Augood SJ, et al., 2003. Distribution and ultrastructural localization of torsinA immunoreactivity in the human brain. Brain Res. 986, 12–21. [PubMed: 12965225]

Augood SJ, et al., 1999. Distribution of the mRNAs encoding torsinA and torsinB in the normal adult human brain. Ann Neurol. 46, 761–9. [PubMed: 10553994]

Augood SJ, et al., 1998. Expression of the early-onset torsion dystonia gene (DYT1) in human brain. Ann Neurol. 43, 669–73. [PubMed: 9585364]

Balcioglu A, et al., 2007. Dopamine release is impaired in a mouse model of DYT1 dystonia. J Neurochem. 102, 783–8. [PubMed: 17550429]

Beauvais G, et al., 2018. Exploring the Interaction Between eIF2alpha Dysregulation, Acute Endoplasmic Reticulum Stress and DYT1 Dystonia in the Mammalian Brain. Neuroscience. 371, 455–468. [PubMed: 29289717]

Bello EP, et al., 2011. Cocaine supersensitivity and enhanced motivation for reward in mice lacking dopamine D2 autoreceptors. Nat Neurosci. 14, 1033–8. [PubMed: 21743470]

Berman BD, et al., 2013. Striatal dopaminergic dysfunction at rest and during task performance in writer's cramp. Brain. 136, 3645–58. [PubMed: 24148273]

Brimblecombe KR, et al., 2015. Gating of dopamine transmission by calcium and axonal N-, Q-, T- and L-type voltage-gated calcium channels differs between striatal domains. J Physiol. 593, 929–46. [PubMed: 25533038]

Burke RE, et al., 1986. Torsion dystonia: a double-blind, prospective trial of high-dosage trihexyphenidyl. Neurology. 36, 160–4. [PubMed: 3511401]

Carbon M, et al., 2009. Abnormal striatal and thalamic dopamine neurotransmission: Genotype-related features of dystonia. Neurology. 72, 2097–103. [PubMed: 19528516]

Cascalho A, et al., 2020. Excess Lipin enzyme activity contributes to TOR1A recessive disease and DYT-TOR1A dystonia. Brain. 143, 1746–1765. [PubMed: 32516804]

Chen P, et al., 2010. The early-onset torsion dystonia-associated protein, torsinA, is a homeostatic regulator of endoplasmic reticulum stress response. Hum Mol Genet. 19, 3502–15. [PubMed: 20584926]

Cornett EM, et al., 2017. Medication-Induced Tardive Dyskinesia: A Review and Update. Ochsner J. 17, 162–174. [PubMed: 28638290]

Correll CU, et al., 2017. Epidemiology, Prevention, and Assessment of Tardive Dyskinesia and Advances in Treatment. J Clin Psychiatry. 78, 1136–1147. [PubMed: 29022654]

Downs AM, et al., 2019. Trihexyphenidyl rescues the deficit in dopamine neurotransmission in a mouse model of DYT1 dystonia. Neurobiol Dis. 125, 115–122. [PubMed: 30707939]

Egami K, et al., 2007. Basal ganglia dopamine loss due to defect in purine recycling. Neurobiol Dis. 26, 396–407. [PubMed: 17374562]

Eskow Jaunarajs KL, et al., 2015. Striatal cholinergic dysfunction as a unifying theme in the pathophysiology of dystonia. Prog Neurobiol. 127–128, 91–107.

Eskow Jaunarajs KL, et al., 2019. Diverse Mechanisms Lead to Common Dysfunction of Striatal Cholinergic Interneurons in Distinct Genetic Mouse Models of Dystonia. J Neurosci. 39, 7195–7205. [PubMed: 31320448]

Fan X, et al., 2018. Dopamine Receptor Agonist Treatment of Idiopathic Dystonia: A Reappraisal in Humans and Mice. J Pharmacol Exp Ther. 365, 20–26. [PubMed: 29348266]

Furukawa Y, et al., 2000. Striatal dopamine in early-onset primary torsion dystonia with the DYT1 mutation. Neurology. 54, 1193–5. [PubMed: 10720299]

Furukawa Y, et al., 1996. GTP-cyclohydrolase I gene mutations in hereditary progressive and dopa-responsive dystonia. Ann Neurol. 39, 609–17. [PubMed: 8619546]

Gonzales KK, Smith Y, 2015. Cholinergic interneurons in the dorsal and ventral striatum: anatomical and functional considerations in normal and diseased conditions. Ann N Y Acad Sci. 1349, 1–45. [PubMed: 25876458]

Gonzalez-Alegre P, Paulson HL, 2004. Aberrant cellular behavior of mutant torsinA implicates nuclear envelope dysfunction in DYT1 dystonia. J Neurosci. 24, 2593–601. [PubMed: 15028751]

Goodchild RE, et al., 2015. Access of torsinA to the inner nuclear membrane is activity dependent and regulated in the endoplasmic reticulum. J Cell Sci. 128, 2854–65. [PubMed: 26092934]

Goodchild RE, Dauer WT, 2004. Mislocalization to the nuclear envelope: an effect of the dystonia-causing torsinA mutation. Proc Natl Acad Sci U S A. 101, 847–52. [PubMed: 14711988]

Goodchild RE, et al., 2005. Loss of the dystonia-associated protein torsinA selectively disrupts the neuronal nuclear envelope. Neuron. 48, 923–32. [PubMed: 16364897]

Granata A, et al., 2008. The dystonia-associated protein torsinA modulates synaptic vesicle recycling. J Biol Chem. 283, 7568–79. [PubMed: 18167355]

Grillet M, et al., 2016. Torsins Are Essential Regulators of Cellular Lipid Metabolism. Dev Cell. 38, 235–47. [PubMed: 27453503]

Grundmann K, et al., 2007. Overexpression of human wildtype torsinA and human DeltaGAG torsinA in a transgenic mouse model causes phenotypic abnormalities. Neurobiol Dis. 27, 190–206. [PubMed: 17601741]

Hewett J, et al., 2000. Mutant torsinA, responsible for early-onset torsion dystonia, forms membrane inclusions in cultured neural cells. Hum Mol Genet. 9, 1403–13. [PubMed: 10814722]

Hewett JW, et al., 2007. Mutant torsinA interferes with protein processing through the secretory pathway in DYT1 dystonia cells. Proc Natl Acad Sci U S A. 104, 7271–6. [PubMed: 17428918]

Hintiryan H, et al., 2016. The mouse cortico-striatal projectome. Nat Neurosci. 19, 1100–14. [PubMed: 27322419]

Ichinose H, Nagatsu T, 1999. Molecular genetics of DOPA-responsive dystonia. Adv Neurol. 80, 195–8. [PubMed: 10410721]

Kile BM, et al., 2010. Synapsins differentially control dopamine and serotonin release. J Neurosci. 30, 9762–70. [PubMed: 20660258]

Koeltzow TE, et al., 1998. Alterations in dopamine release but not dopamine autoreceptor function in dopamine D3 receptor mutant mice. J Neurosci. 18, 2231–8. [PubMed: 9482807]

Koh JY, et al., 2013. Dystonia-associated protein torsinA is not detectable at the nerve terminals of central neurons. Neuroscience. 253, 316–29. [PubMed: 24025868]

Kumar A, et al., 2015. GDNF Overexpression from the Native Locus Reveals its Role in the Nigrostriatal Dopaminergic System Function. PLoS Genet. 11, e1005710. [PubMed: 26681446]

Kurian MA, et al., 2011. Clinical and molecular characterisation of hereditary dopamine transporter deficiency syndrome: an observational cohort and experimental study. Lancet Neurol. 10, 54–62. [PubMed: 21112253]

Lester DB, et al., 2010. Acetylcholine-dopamine interactions in the pathophysiology and treatment of CNS disorders. CNS Neurosci Ther. 16, 137–62. [PubMed: 20370804]

Lopes EF, et al., 2019. Inhibition of Nigrostriatal Dopamine Release by Striatal GABAA and GABAB Receptors. J Neurosci. 39, 1058–1065. [PubMed: 30541909]

Mehta SH, et al., 2015. Drug-induced movement disorders. Neurol Clin. 33, 153–74. [PubMed: 25432728]

Misbahuddin A, et al., 2005. Mutant torsinA, which causes early-onset primary torsion dystonia, is redistributed to membranous structures enriched in vesicular monoamine transporter in cultured human SH-SY5Y cells. Mov Disord. 20, 432–40. [PubMed: 15593317]

Oberlin SR, et al., 2004. Development and anatomic localization of torsinA. Adv Neurol. 94, 61–5. [PubMed: 14509655]

Ozelius LJ, et al., 1997. The early-onset torsion dystonia gene (DYT1) encodes an ATP-binding protein. Nat Genet. 17, 40–8. [PubMed: 9288096]

Ozelius LJ, et al., 1992. Strong allelic association between the torsion dystonia gene (DYT1) andloci on chromosome 9q34 in Ashkenazi Jews. Am J Hum Genet. 50, 619–28. [PubMed: 1347197]

Page ME, et al., 2010. Cell-autonomous alteration of dopaminergic transmission by wild type and mutant (DeltaE) TorsinA in transgenic mice. Neurobiol Dis. 39, 318–26. [PubMed: 20460154]

Pappas SS, et al., 2018. A cell autonomous torsinA requirement for cholinergic neuron survival and motor control. Elife. 7.

Pelosi A, et al., 2017. Heterozygous Gnal Mice Are a Novel Animal Model with Which to Study Dystonia Pathophysiology. J Neurosci. 37, 6253–6267. [PubMed: 28546310]

Pisani A, et al., 2006. Altered responses to dopaminergic D2 receptor activation and N-type calcium currents in striatal cholinergic interneurons in a mouse model of DYT1 dystonia. Neurobiol Dis. 24, 318–25. [PubMed: 16934985]

Puglisi F, et al., 2013. Torsin A Localization in the Mouse Cerebellar Synaptic Circuitry. PLoS One. 8, e68063. [PubMed: 23840813]

Rice ME, Cragg SJ, 2004. Nicotine amplifies reward-related dopamine signals in striatum. Nat Neurosci. 7, 583–4. [PubMed: 15146188]

Rilstone JJ, et al., 2013. Brain dopamine-serotonin vesicular transport disease and its treatment. N Engl J Med. 368, 543–50. [PubMed: 23363473]

Rizzi G, Tan KR, 2017. Dopamine and Acetylcholine, a Circuit Point of View in Parkinson's Disease. Front Neural Circuits. 11, 110. [PubMed: 29311846]

Roberts BM, et al., 2020. GABA uptake transporters support dopamine release in dorsal striatum with maladaptive downregulation in a parkinsonism model. Nat Commun. 11, 4958. [PubMed: 33009395]

Scarduzio M, et al., 2017. Strength of cholinergic tone dictates the polarity of dopamine D2 receptor modulation of striatal cholinergic interneuron excitability in DYT1 dystonia. Exp Neurol. 295, 162–175. [PubMed: 28587876]

Sciamanna G, et al., 2009. Impaired striatal D2 receptor function leads to enhanced GABA transmission in a mouse model of DYT1 dystonia. Neurobiol Dis. 34, 133–45. [PubMed: 19187797]

Sciamanna G, et al., 2012a. Cholinergic dysregulation produced by selective inactivation of the dystonia-associated protein torsinA. Neurobiol Dis. 47, 416–27. [PubMed: 22579992]

Sciamanna G, et al., 2012b. Cholinergic dysfunction alters synaptic integration between thalamostriatal and corticostriatal inputs in DYT1 dystonia. J Neurosci. 32, 11991–2004. [PubMed: 22933784]

Simonyan K, et al., 2013. Abnormal striatal dopaminergic neurotransmission during rest and task production in spasmodic dysphonia. J Neurosci. 33, 14705–14. [PubMed: 24027271]

Song CH, et al., 2012. Functional analysis of dopaminergic systems in a DYT1 knock-in mouse model of dystonia. Neurobiol Dis. 48, 66–78. [PubMed: 22659308]

Threlfell S, et al., 2010. Striatal muscarinic receptors promote activity dependence of dopamine transmission via distinct receptor subtypes on cholinergic interneurons in ventral versus dorsal striatum. J Neurosci. 30, 3398–408. [PubMed: 20203199]

Threlfell S, Cragg SJ, 2011. Dopamine signaling in dorsal versus ventral striatum: the dynamic role of cholinergic interneurons. Front Syst Neurosci. 5, 11. [PubMed: 21427783]

Tolosa E, Compta Y, 2006. Dystonia in Parkinson's disease. J Neurol. 253 Suppl 7, Vii7–13. [PubMed: 17131231]

Torres GE, et al., 2004. Effect of torsinA on membrane proteins reveals a loss of function and a dominant-negative phenotype of the dystonia-associated DeltaE-torsinA mutant. Proc Natl Acad Sci U S A. 101, 15650–5. [PubMed: 15505207]

Weisheit CE, Dauer WT, 2015. A novel conditional knock-in approach defines molecular and circuit effects of the DYT1 dystonia mutation. Hum Mol Genet. 24, 6459–72. [PubMed: 26370418]

Wichmann T, 2008. Commentary: Dopaminergic dysfunction in DYT1 dystonia. Exp Neurol. 212, 242–6. [PubMed: 18513716]

Wijemanne S, Jankovic J, 2015. Dopa-responsive dystonia--clinical and genetic heterogeneity. Nat Rev Neurol. 11, 414–24. [PubMed: 26100751]

Yan Z, et al., 1997. D2 dopamine receptors reduce N-type Ca2+ currents in rat neostriatal cholinergic interneurons through a membrane-delimited, protein-kinase-C-insensitive pathway. J Neurophysiol. 77, 1003–15. [PubMed: 9065864]

Yorgason JT, et al., 2011. Demon voltammetry and analysis software: analysis of cocaine-induced alterations in dopamine signaling using multiple kinetic measures. J Neurosci Methods. 202, 158–64. [PubMed: 21392532]

Zhang L, et al., 2009. Controls of tonic and phasic dopamine transmission in the dorsal and ventral striatum. Mol Pharmacol. 76, 396–404. [PubMed: 19460877]

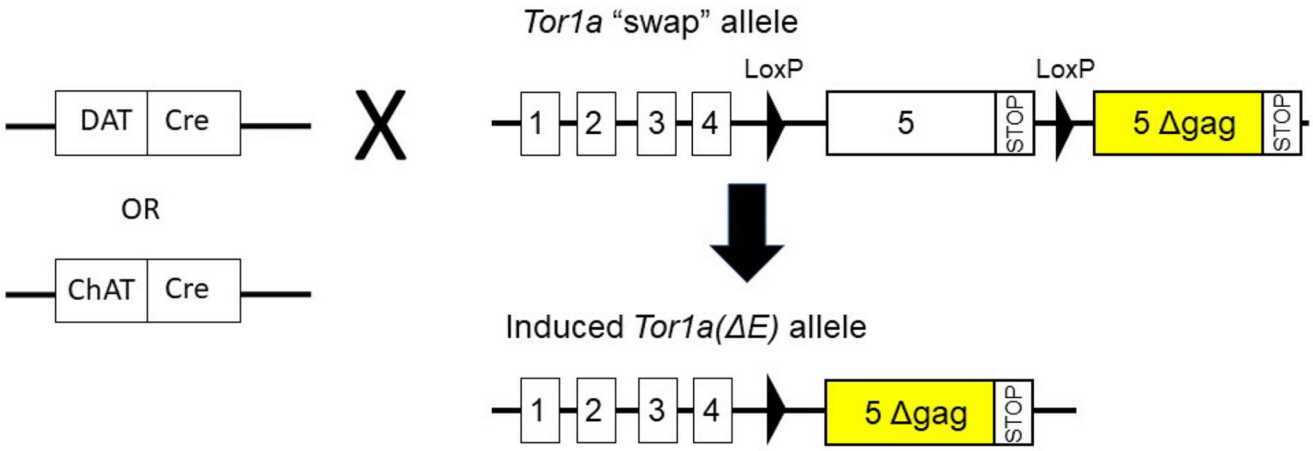

Fig 1. Schematic of cell-type specific *Tor1a(ΔE)* knockin approach.

Mice carrying the "swap" allele were crossed with either ChAT-cre or DAT-cre expressing mice to selective express *Tor1a(ΔE)* in ChAT+ or DAT+ neurons respectively.

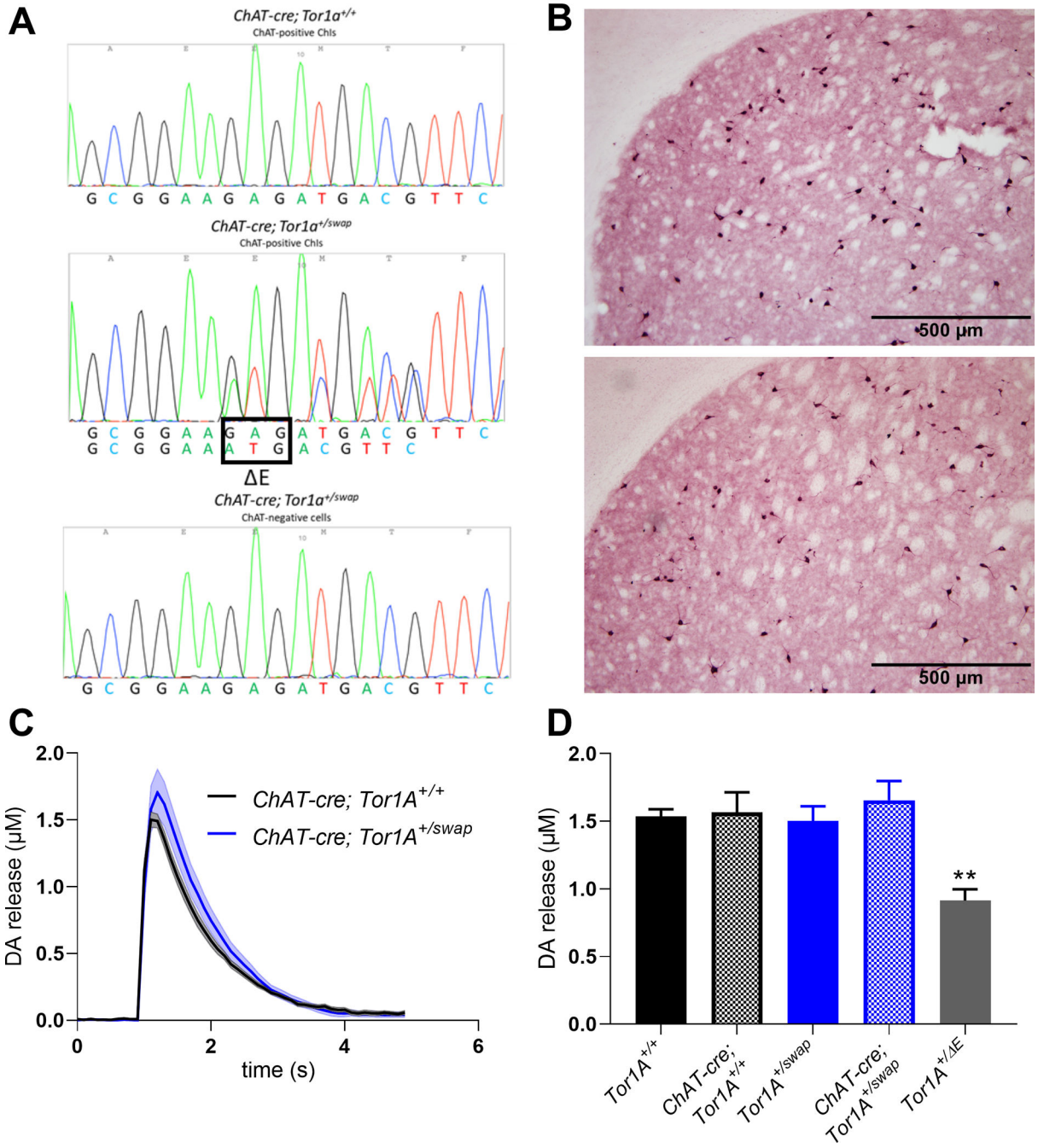

Fig 2. Expression of *Tor1a(ΔE)* in ChAT+ neurons does not alter DA release.

(**A**) Validation of cell-type specific expression of *Tor1a(ΔE)* in striatal cholinergic cells. Sequencing traces demonstrate that *ChAT-cre; Tor1a*$^{+/swap}$ mice express one copy of the *Tor1a(ΔE)* mutation in cholinergic cells but not ChAT-negative cells in the striatum. Cholinergic cells from *ChAT-cre; Tor1a*$^{+/+}$ do not express *Tor1a(ΔE).* (**B**) Immunostaining for ChAT in the striatum. There is no obvious change in the number or distribution of striatal ChIs in either *ChAT-cre; Tor1a*$^{+/+}$ (upper figure) or *ChAT-cre; Tor1a*$^{+/swap}$ mice (lower figure). (**C**) Striatal DA release is unchanged in *ChAT-cre; Tor1a*$^{+/swap}$ versus *ChAT-cre;*

Tor1a$^{+/+}$ (n= 5). (**D**) Striatal DA release is significantly reduced in *Tor1a*$^{+/\Delta E}$ versus all other genotypes (n = 5 for all except *Tor1a*$^{+/\Delta E}$, n = 17). Values represent mean ± SEM.

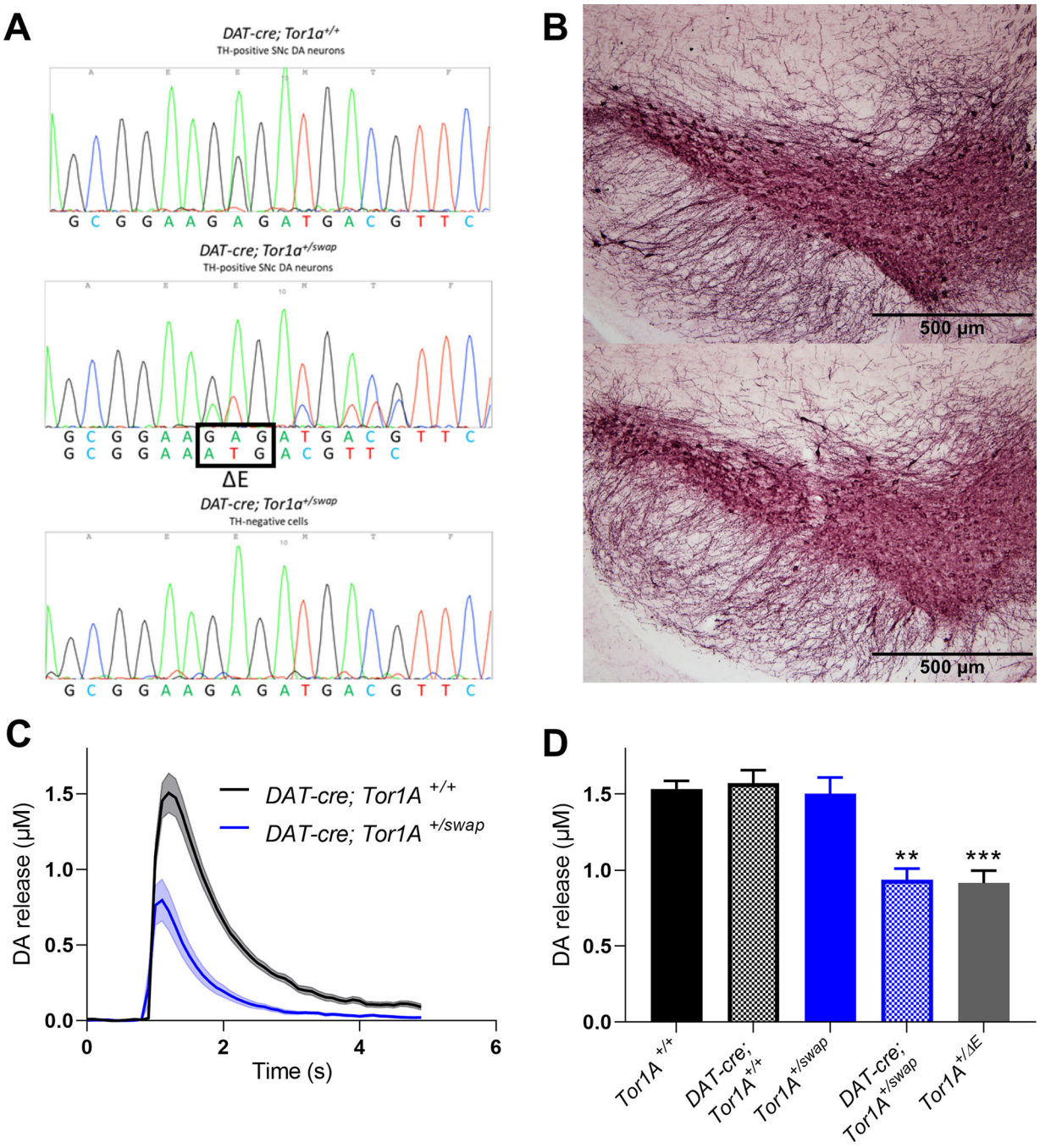

Fig 3. Expression of *Tor1a(ΔE)* in DA neurons reduces striatal DA release.

(**A**) Validation of cell-type specific expression of *Tor1a(ΔE)* in SNc DA neurons. Sequencing traces demonstrate that *DAT-cre; Tor1a*$^{+/swap}$ mice express one copy of the *Tor1a(ΔE)* mutation in SNc DA neurons but not TH-negative cells in the midbrain. SNc DA neurons from *DAT-cre; Tor1a*$^{+/+}$ do not express *Tor1a(ΔE).* (**B**) Immunostaining for TH in the SNc. There is no obvious change in the number or distribution of SNc DA neurons in either *DAT-cre; Tor1a*$^{+/+}$ (upper figure) or *DAT-cre; Tor1a*$^{+/swap}$ mice (lower figure). (**C**) Striatal DA release is significantly reduced in *DAT-cre; Tor1a*$^{+/swap}$ versus *DAT-cre; Tor1a*$^{+/+}$ (n= 5). (**D**)

Striatal DA release is reduced in both *DAT-cre; Tor1a*$^{+/swap}$ and Tor1a$^{+/\Delta E}$ versus all control genotypes. DA release is not significantly different between *DAT-cre; Tor1a*$^{+/swap}$ and *Tor1a*$^{+/\Delta E}$ (n = 5 for all except *Tor1a*$^{+/\Delta E}$, n = 17). Values represent mean ± SEM).

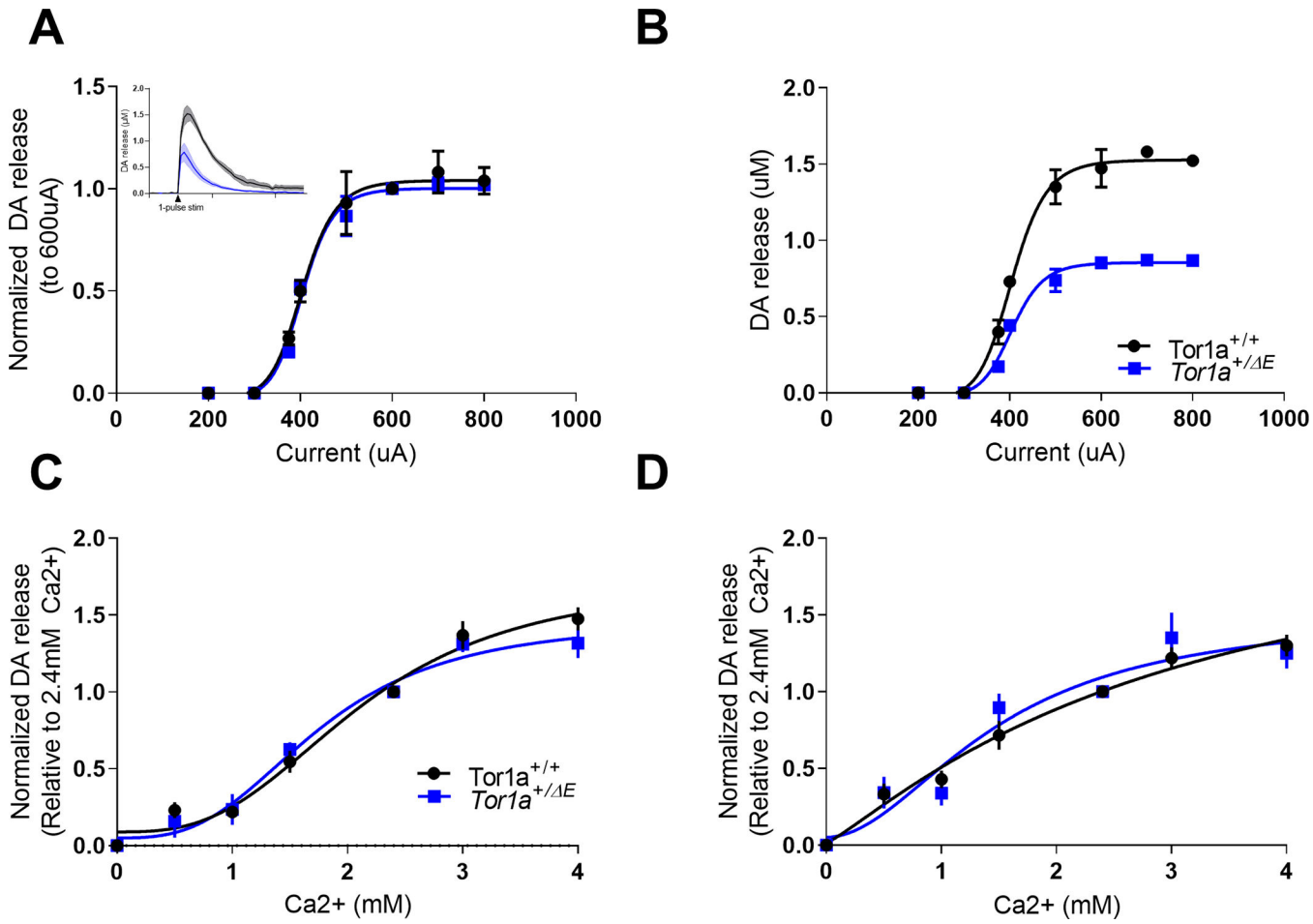

Fig 4. Sensitivity of striatal DA release to increasing stimulation current and extracellular Ca^{2+}.

(**A**) There is no difference in the sensitivity of DA release to electrical stimulation of increasing current. There is no significant difference in EC_{50} between control and *Tor1a*$^{+/\Delta E}$ mice ($n = 3$). (**A inset**) DA release traces after single-pulse 600 μA electrical stimulation in *Tor1a*$^{+/\Delta E}$ KI and control mice. (**B**) Increasing stimulation current does not normalize DA release in *Tor1a*$^{+/\Delta E}$ mice to control levels ($n = 3$). (**C**) Control and *Tor1a*$^{+/\Delta E}$ mice have similar sensitivity to varying concentrations of Ca^{2+} after 1-pulse electrical stimulation. There was no significant difference in EC_{50} between control and *Tor1a*$^{+/\Delta E}$ ($n = 6$). (**D**) Control and *Tor1a*$^{+/\Delta E}$ mice have similar sensitivity to varying concentrations of Ca^{2+} after 5-pulse 100 hz electrical stimulation. There was no significant difference in EC_{50} between control and *Tor1a*$^{+/\Delta E}$ mice ($n = 6$). Values represent mean ± SEM.

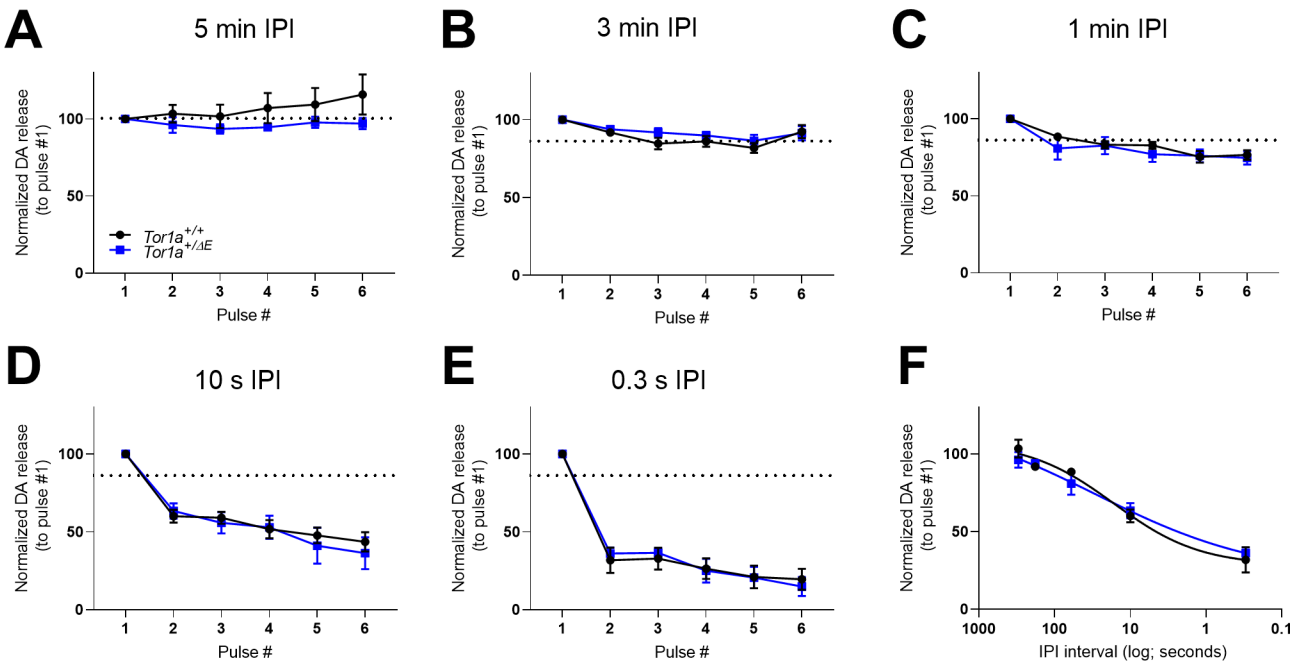

Fig 5. Rundown of evoked DA release after repeated simulation.

DA release was recorded after sequential electrical stimulations with varying inter-pulse intervals (IPI) of 5 min (**A**), 3 min (**B**), 1 min (**C**), 10 sec (**D**), and 0.3 sec (**E**). (**F**) DA release at the second pulse normalized to the first pulse for all inter-pulse intervals (IPI) tested. There was no significant effect of genotype observed at any IPI ($n = 6$). Values represent mean ± SEM.

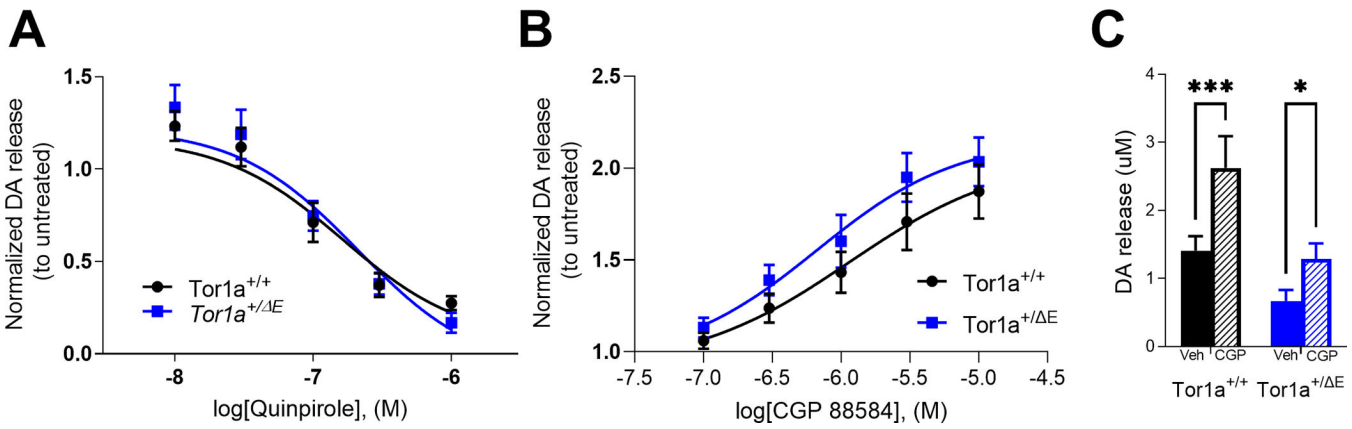

Fig 6. Sensitivity of *Tor1a*$^{+/\Delta E}$ mice to D2 receptor activation or $GABA_B$ receptor blockade.

(**A**) Control and *Tor1a*$^{+/\Delta E}$ mice have similar sensitivity to the D2 DA receptor agonist quinpirole. There was no significant difference in IC_{50} between control and *Tor1a*$^{+/\Delta E}$ mice ($n = 5$). (**B**) $GABA_B$ receptor function in *Tor1a*$^{+/\Delta E}$ mice. *Tor1a*$^{+/+}$ and *Tor1a*$^{+/\Delta E}$ mice have similar sensitivity to the $GABA_B$ receptor antagonist CGP 88584. There was no significant difference in EC_{50} between *Tor1a*$^{+/+}$ and *Tor1a*$^{+/\Delta E}$ mice ($n = 5$). (**C**) Maximal effect of CGP 88584 (10 μM) on DA release. CGP 88584 significantly enhanced DA release in both genotypes, but there was no significant difference between the genotypes. Values represent mean ± SEM.

Table 1

Tissue monoamines in the striatum

	Tor1A$^{+/swap}$	**DAT-cre; Tor1A$^{+/+}$**	**DAT-cre; Tor1A$^{+/swap}$**	**ChAT-cre; Tor1A$^{+/+}$**	**ChAT-cre; Tor1A$^{+/swap}$**
DA	37.01±4.69	29.15±3.07	37.75±5.60	42.84±4.05	43.56±5.85
DOPAC	1.96±0.31	1.71±0.34	2.02±0.39	1.85±0.12	1.93±0.32
HVA	3.20±0.39	3.32±0.34	4.02±0.91	3.77±0.30	3.70±0.62
3-MT	1.73±0.20	1.71±0.19	2.33±0.46	1.97±0.23	2.03±0.27